Journal of Metals, Materials and Minerals. Vol.19 No.1 pp.29-38, 2009

Determination of Yield Behaviour of Boron Alloy Steel at High Temperature

Jennarong TUNGTRONGPAIROJ[1], Vitoon UTHAISANGSUK[2] and Wolfgang BLECK[2]

[1]The Sirindhorn International Thai-German School of Engineering, King Mongkut's University of Technology North Bangkok (KMUTNB), 1518, Pibulsongkram Rd., Bangsue, Bangkok 10800, Thailand
[2]Department of Ferrous Metallurgy, RWTH Aachen University, Intzestr.1,52072, Germany

Received Jan. 12, 2009
Accepted Apr. 8, 2009

Abstract

The hot tensile test is a basic material testing method for investigation of the mechanical properties of steel at high temperature conditions. In industrial hot sheet forming processes such as hot stamping and hot gas metal forming, the influences of temperature and strain rate on microstructure and material behaviour play a significant role. In this work, sheet samples of steel grade 22MnB5 were examined using a hot deformation simulator. Different temperatures between 900 and 1200°C, which are above A_{c3}, and strain rates between 0.001 and 0.1 s^{-1} were considered. During the tensile test, a laser speckle extensometer (LSE) was deployed for measuring the local strain values on the deformed sample. By means of this LSE, more accurate stress-strain responses were obtained. Reliable flow curves are indispensable data for simulations of the hot forming processes. The influences of temperature and strain rate on the plastic behaviour of the boron steel were investigated. From temperature higher than 900°C, the flow stresses explicitly decrease and the formability enhances. Due to the martensitic transformation during a fast cooling the strength of this steel is improved. A fully martensitic microstructure with a small amount of retained austenite was observed in the samples after the hot tensile test and a typical ductile fracture was detected.

Key words : Hot tensile test, 22MnB5, Stress-strain curve, Strain rate

Introduction

Manufacturing technologies for metal have been greatly and rapidly developed in recent years. For sheet metal working, hot stamping, hot gas metal forming and incremental sheet forming with local heating are nowadays in focus. In the hot forming process, temperature and strain rate have considerable effects on the material behaviour with regards to the microstructure changing, recry-stallisation and strain softening. The investigation of material behaviour at high temperature is therefore necessary. The boron alloy steel 22MnB5 is commonly processed in the hot forming. 22MnB5 is an ultra-high strength steel that has good hardenability and formability. The strength of post-formed part of this steel can be improved due to the martensitic transformation by cooling down. Its yield strength and ultimate tensile strength can be increased to 1000 and 1500 MPa, respectively, after hot stamping.(1) The mostimportant element in this steel is boron. Boron promotes a strong hardening, a quite good wear, and abrasion resistance after quenching. Steel with thirty ppm of boron has the same hardness properties as steel with a composition of 0.6%Mn, 0.7%Cr, 0.5%Mo or 1.5% Ni.(2) Boron delays the ferrite and pearlite transformations during the processing while the martensite and bainite transformation is not influenced, Figure 1.(3) It also leads to boron segregation on the austenite grain boundaries.(4, 5) Most boron steel grades are usually applied in car chassis parts. The advantages of the hot stamping process of the boron steel are 1) very high formability during hot forming, 2) forming of very complex geometries, 3) producing of ultra-high strength steel parts, 4) high toughness, 5) independence of material properties on the forming depth, 6) acceptable dimensional tolerances, 7) good weldability and 8) crash application.(6)

E-mail: tung_jenn@hotmail.com, uthai@iehk.rwth-aachen.de, bleck@iehk.rwth-aachen.de

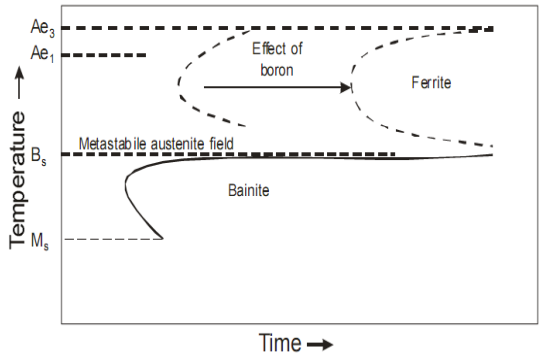

Figure 1. Schematic representation of the influence of boron on the phase transformation behaviour.[3]

The factors affecting the hardenability of boron steel are 1) austenitizing time and temperature, 2) austenite grain size, 3) pre-forming and heat treatment, and 4) the other alloying elements. If the percentage of carbon is higher, the boron hardenability effect will decrease. Boron is most effective in increasing the hardenability of low carbon steels and does not take effect in steel with carbon content higher than 0.8 percent (Figure 2). For instance, it was shown in (Kapadia, 1977) that boron is usually added to increase the hardenability of low carbon steel.

As-delivered boron steel presents a tensile strength of approximately 600 MPa. Ferrite, pearlite and some carbides are typical constituents in the initial microstructure. After the hot stamping, the strength can increase up to 1500 MPa because the final microstructure exhibits only lath martensite or lath martensite with small amounts of bainite and retained austenite.

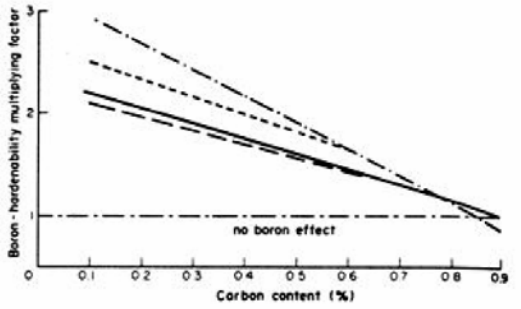

Figure 2. Hardenability of boron with percentage of carbon in plain carbon and low alloy steels.[7]

The previous work of Naderi, *et al.*(2008), constitutive relationships for 22MnB5 boron steel deformed isothermally at high temperatures, showed that the forming temperature is a significant factor that influences the stress level of the flow curve. The flow stress of material at low forming temperature is definitely higher than the one at high forming temperature. In addition, the flow stress also increases when increasing strain rate, Figure 3. Besides, (Turetta, *et al.* 2006) investigated the formability of 22MnB5 in hot stamping operation. The non-isothermal uniaxial tensile tests were carried out with subsequently quenching the specimen. The results showed that the temperature has a strong effect while the strain rate seems to have less influence on the material process window, Figure 4.

In this work, the determination of flow curve of the boron steel 22MnB5 at temperature higher than the A_{c3} using a hot tensile testing in combination with numerical simulation is the main objective. Some results from the FE simulations of the hot tensile test will be shown in comparison with the experimental results. The aim of this comparison is to verify the prediction of the stress-strain curves. In the experimental tensile test, the average cross head speeds of the machine was typically used to set the corresponding strain rate. The local strain by the tensile test at high temperature is non-uniform so that it can lead to an inhomogeneous material property. These results will also be discussed with regards to the investigation of microstructure and fracture behaviour.

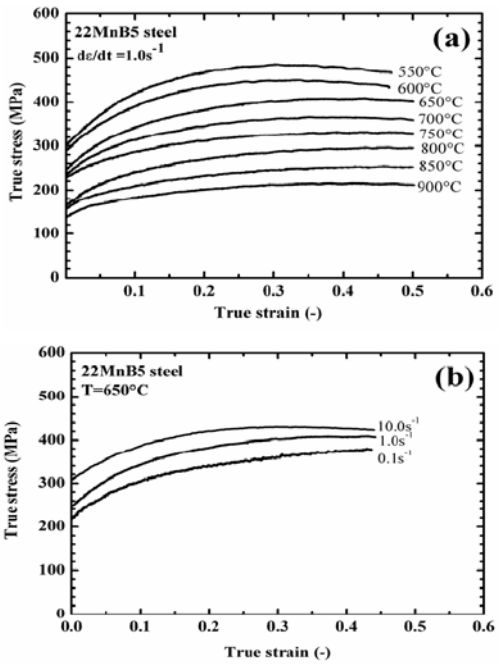

Figure 3. Flow curves of 22MnB5 steel determined from isothermal compression test, (a) at different deformation temperatures with strain rate of 1.0 s^{-1}, and (b) at deformation temperature of 650°C and with different strain rates.[8]

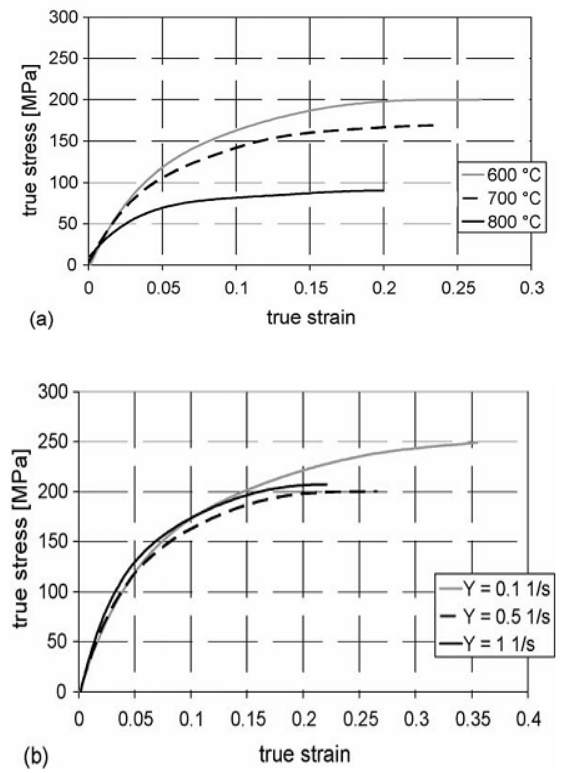

Figure 4. Flow curves of 22MnB5 steel determined from non-isothermal tensile test, (a) at different deformation temperatures with strain rate of 0.5 s^{-1}, and (b) at deformation temperature of 600°C and with different strain rates.[9]

During the tensile tests, the local strain was directly measured on the sample by means of a Laser Speckle Extensometer (LSE). The effective strain rate for each forming condition can then be determined. Comparisons of these data with results from FE simulations of the hot tensile test were used to adjust the effective forming velocity. By this way, the accuracy of the determined flow curve in hot tensile testing will be improved.

In industry, forming processes mostly take place at a constant machine speed. In this experiment, hot tensile tests were performed at constant strain rates and constant cross head speeds. The results showing the stress-strain responses and the local strain rates were compared for both conditions. The hot tensile test using constant cross head speeds provided flow curves close to those from the tests using a constant strain rate. However, large scatters were found for the local strain rate values measured by the LSE, which will be discussed later together with the results from the FE simulations.

Materials and Experimental Procedures

The boron alloy steel 22MnB5 was investigated and the chemical composition of this steel is shown in Table 1. Many sources show that this steel grade has a very high strength value after hot forming. The hardness and tensile strength depend on the carbon content. Boron in 22MnB5 steel acts as a hardenability enhancer. In (Kapadia, 1978 and Morral and Cameron, 1980) it was mentioned that the addition of typically 10-30 ppm of boron to different low alloy steel grades causes the segregation of boron on the austenite grain boundaries, which delays the nucleation of ferrite.

Table 1. Chemical composition of investigated material (values in weight %)[10]

	C	Si	Mn	Ni	Cr	P
22MnB5	0.226	0.269	1.200	-	-	0.013
	S	**N**	**Al**	**Nb**	**Ti**	**B**
	0.003	0.006	0.029	0.001	0.039	0.0035

The sheet sample dimension applied for the hot tensile test is 170, 8, and 1.5 mm in length, width, and thickness, respectively. The specimen was located in a vacuum chamber of the hot deformation simulator (Figure 5). Thermocouples were welded in the middle of the sample to measure and control the temperature. The induction coil was used for heating-up the sample. At the start of the experiments, argon or helium gas was blown into the chamber. The specimen was heated up at a rate of 6 K/s. After a short holding time of 30 seconds the sample was tensioned until fracture, and then cooled down at an approximate rate of 10 K/s by air, Figure 6 (a). In this work, some specimens were only heated (6 K/s) and cooled rapidly (200 K/s) by inert gas like helium or argon to observe the austenitic grain size and microstructure before deformation at different test temperatures, Figure 6 (b). The LSE was applied to measure the local strain values on the samples during deformation. The LSE consists of two lasers and two cameras. These two lasers beam to the surface of the specimen and capture its surface topology. To measure the displacement of the sample, the movement of the speckle pattern was traced.

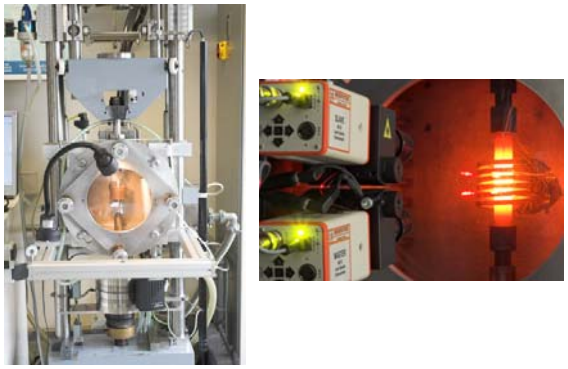

Figure 5. Hot deformation simulator and the LSE

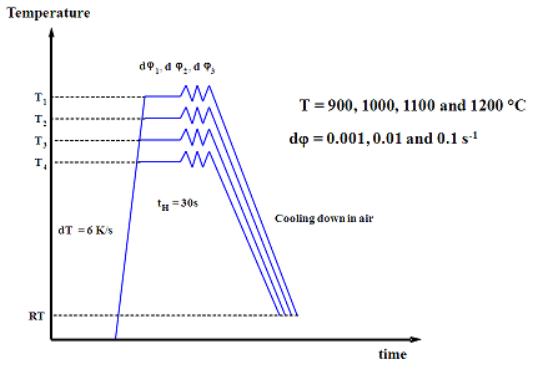

(a)

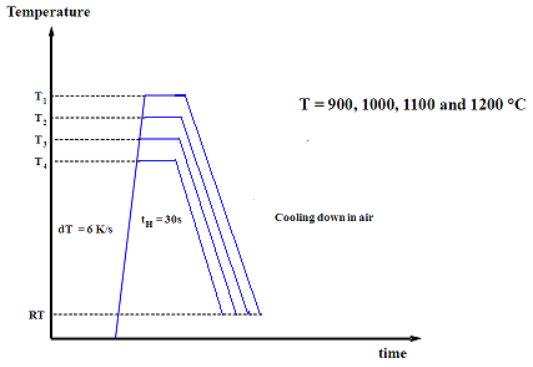

(b)

Figure 6. (a) Hot tensile test programme[10] and (b) Heat treatment programme with fast cooling down (200 K/s)

ABAQUS was used to simulate the hot tensile test in this work. The plastic true stress-strain data from the experiment are the most important input data for the FE simulations. The other required material parameters are the density, heat transfer coefficient, and heat conductivity. Furthermore, the total simulation time corresponding to the cross head speeds of the machine were given in order to regulate the strain rate.

The simulations were performed under uniaxial tensile loading and isothermal condition. The temperature on the sample was kept constant during the forming step. Due to the symmetry condition a one-eighth of the tensile specimen was modelled. By using this model the calculation time is reduced. In this case, during the result evaluation force values must be multiplied by four and displacement values by two because of the simplified model. A thermal linear brick element type of C3D8T was used. As no damage model was applied to the simulation, the results after the numerical necking of the sample could not be correctly predicted. Thus, the experimental and calculated stress-strain curves can be compared until this point.

In the experimental hot tensile test, the overall strain rate was controlled only by the cross head speeds of the machine. In the FEM simulation, an average tension rate was identified first. These average values were used as a correction factor to set the simulation times, which are in accordance with the investigated cross head speeds. In this manner, it was assumed that the effect of the inhomogeneous distribution of temperature and the resulting non-uniform local strain rate in the heat-affected zone of the sample were taken into account.

Results & Discussion

During the hot tensile test, the forces and the local strains were recorded. Using these data, engineering stress-strain curves were evaluated, which represent the important mechanical values like the yield strength, ultimate tensile strength, uniform elongation and elongation at fracture. The plastic true stress-strain curve or the flow curves were also evaluated for applying in the simulation.

The Flow Behaviour

The investigated steel 22MnB5 exhibits an identical strain hardening rate at different temperatures, as illustrated by the engineering stress-strain diagrams for a tested strain rate of 0.01 s^{-1} in Figure 7. The flow stress and the formability of the material at temperatures higher than 900°C explicitly decrease.

As mentioned, the strength of the material decreases when the temperature increases. As a result in Figure 7, the tensile strength at 1200˚C is 60 MPa less than the tensile strength at 900˚C. In contrast, the strength increases when the rate of deformation rises which is the same behaviour as shown in (Naderi, *et al.* 2008) and Figure 3. In Figure 8, the tensile strength for the temperature of 1000°C at 0.001 s^{-1} is 40 MPa less than the one at 0.1 s^{-1}.

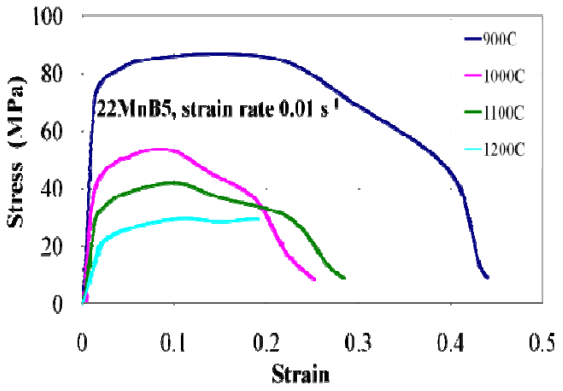

Figure 7. Engineering stress-strain curves of the investigated steel 22MnB5 at the strain rate of 0.01 s^{-1} for different temperatures.

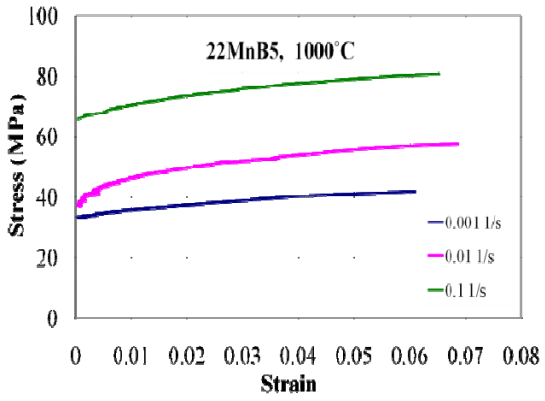

Figure 8. Plastic true stress-strain curves of the investigated steel 22MnB5 at the temperature of 1000°C for different strain rates.

One interesting investigation of this work is the comparison of the results from the hot tensile testing using constant strain rate and constant cross head speed velocity. Figure 9 only shows a small difference between the flow curves in comparison with the hot tensile test using both settings. Note that the cross head speed used in this work was firstly calculated by means of simulation. This means that by the experimental hot tensile test the deformation with defined strain rate can be realised by controlling the cross head speed of the machine.

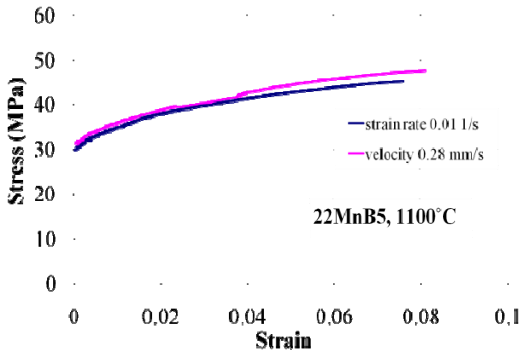

Figure 9. Flow curves of the investigated steel 22MnB5 at 1100°C using constant strain rate of 0.01s^{-1} and constant cross head speeds of 0.28 mm/s.

Figure 10 illustrates the developments of the local strain rate determined by the LSE system for different settings (preset constant strain rate and cross head speed) at 1100°C.

The average local strain rates (Figure 10 (a)) correspond with the defined rates in the middle of the sample in case of preset constant strain rate. In case of constant cross head speed (Figure 10 (b)), the average of the measured local strain rates for 0.28 mm/s underestimates the expected strain rate of 0.01 s^{-1} to a certain extent. It should be mentioned that the measured local strain rate on the sample in hot tensile test is not exactly equal to the given input strain rate. This could be explained by the imprecise data determined by the laser speckle extensometer and the calibration of the preset cross head speed. However, the scatters of the local strain rate are within an acceptable range. Furthermore, in case of very low strain rate the development of the local strain rate using constant strain rate is similar to the one using constant cross head speed, as shown in Figure 10 (c).

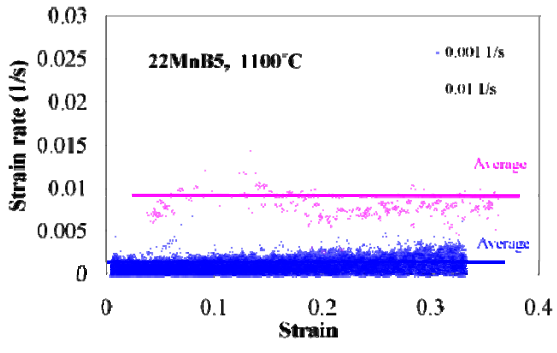

(a)

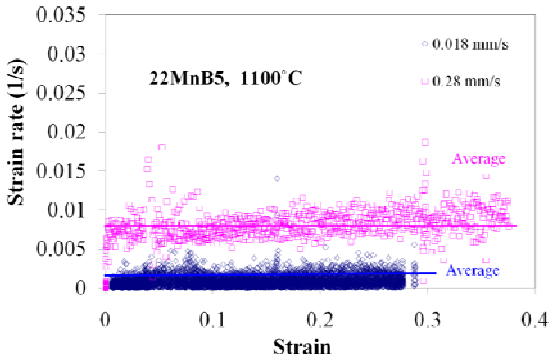

(b)

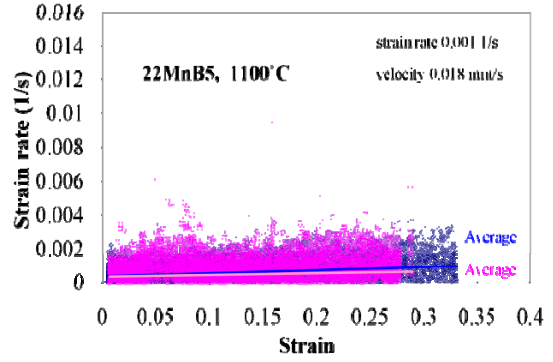

(c)

Figure 10. Development of the local strain rate of the investigated steel 22MnB5 measured by the LSE in the hot tensile test at the temperature of 1100°C, (a) using preset constant strain rate, (b) using preset constant cross head speeds, and (c) comparison of both cases.

Simulation Analysis

The plastic true stress-strain curves determined from the experiments were used as input data for the simulations. The results from the simulation can only be used for comparison up to the beginning of the numerical necking, which is shown as the drop of the force in Figure 11. The experimental and calculated force-displacement curves from the hot tensile test at 1100°C and strain rate of 0.01 s^{-1} are compared in Figure 11. Both curves are similar up to the point of maximum force, and the part of the curve beyond this point was neglected, because the necking process was not considered to be in the scope of this work. The force-displacement curves for other temperatures and strain rates were also calculated. Figure 12 illustrates calculated force-displacement curves of the investigated steel during hot tensile test at temperatures between 900°C and 1100˚C. The trend of the predicted force-displacement curves in this temperature range is reasonable. The calculated plastic strain distributions on the specimens at the total elongation of 0.25 by the tensile tests at strain rate of 0.1 s^{-1} and temperatures between 900°C and 1050°C for the investigated steel are shown in Figure 13.

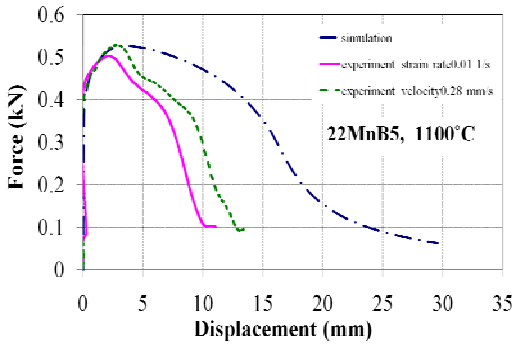

Figure 11. Experimentally determined and calculated force-displacement curves of the investigated steel 22MnB5 during hot tensile test at 1100°C, strain rate of 0.01 s^{-1} and cross head speed of 0.28 mm/s.

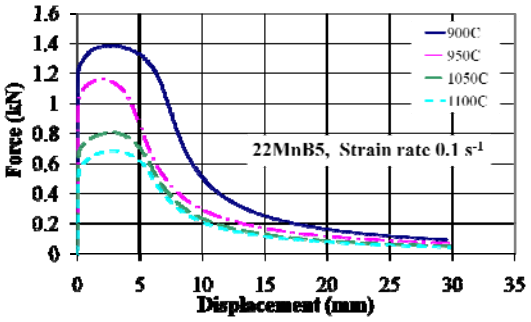

Figure 12. Prediction of force-displacement curves in hot tensile test at temperature between 900°C and 1100°C and strain rate of 0.1 s^{-1} for the investigated steel 22MnB5.

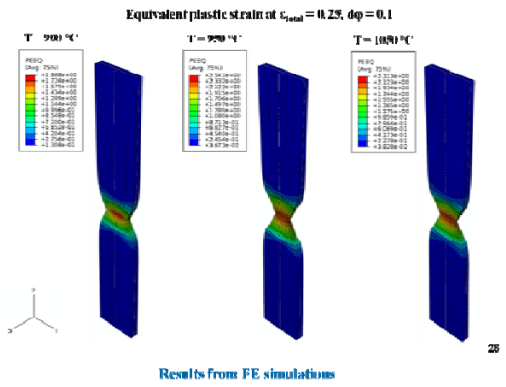

Figure 13. Plastic strain distributions on specimens by tensile tests at strain rate of 0.1 s^{-1} and temperatures between 900°C and 1050°C at the total elongation of 0.25 for the investigated steel 22MnB5.

In addition, tensile tests for the temperature of 1050°C and different strain rates were simulated and the resulting force-displacement curves were calculated, illustrated in Figure 14. Figure 15 depicts the temperature and plastic strain distributions on specimens by tensile tests at temperature of 950°C and strain rate between 0.01 and 0.1 s^{-1} at the total elongation of 0.25 for the investigated steel 22MnB5.

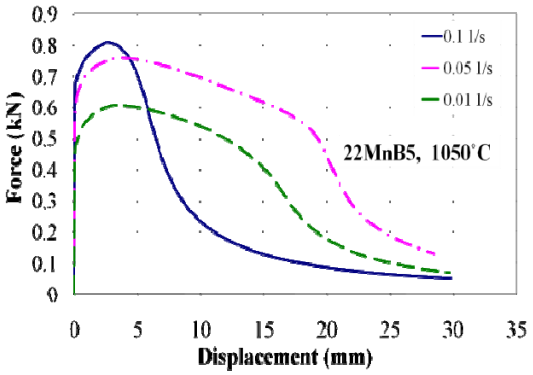

Figure 14. Prediction of force-displacement curves in hot tensile test at temperature of 1050°C and strain rate between 0.01 and 0.1 s^{-1} for steel grade 22MnB5.

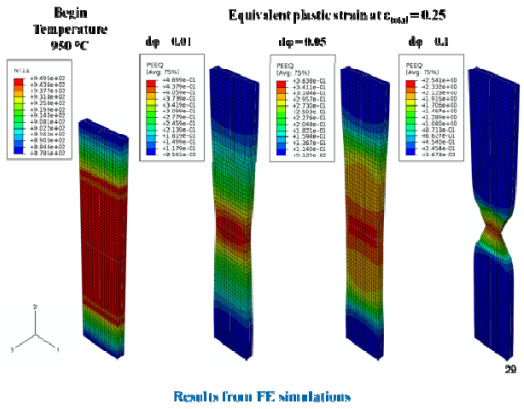

Figure 15. Temperature and plastic strain distributions on specimens by tensile tests at temperature of 950°C and strain rate between 0.01 and 0.1 s^{-1} at the total elongation of 0.25 for the investigated steel 22MnB5.

Microstructure

The as-delivered microstructure shows anisotropic inhomogeneity observed as the secondary microstructural banding of ferritic-pearlitic steel in Figure 16.[3] This structure was caused by cold rolling process and the grains are oriented in the rolling direction, presently a preferred orientation. The ferritic-pearlitic phases are transformed to martensite after hot deformation.

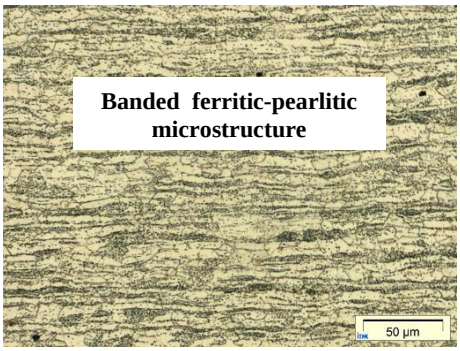

Figure 16. Microstructure of the as-delivered 22MnB5 steel

Additional experiments without forming were carried out to investigate the final microstructure. Samples were austenitized at different temperatures and then cooled down with a cooling rate faster than the one used in the hot tensile test. The resulting microstructures mainly contain fine martensite lath-link with some retained austenite, as shown in Figure 17. By this condition, the material cannot homogeneously solidify, and the growing of the link is thus prevented. Martensite was observed in most areas of the microstructures. The influence of 0.003% boron delays the ferrite-pearlite transformation and subsequently, increasingly promotes the martensite transformation. The austenitization temperature influences the grain growth in the microstructure, but also increases the retained austenite grain size, Figure 17. If the austenitization temperature increases, the martensite start temperature M_s becomes higher.[11]

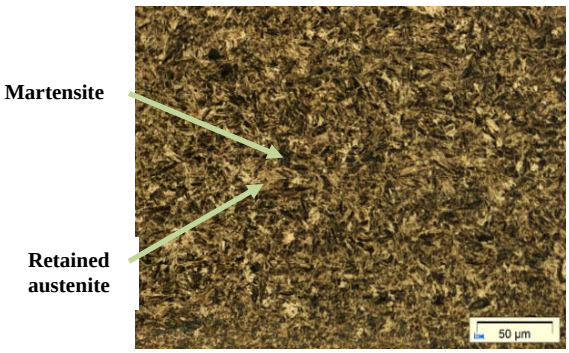

(a)

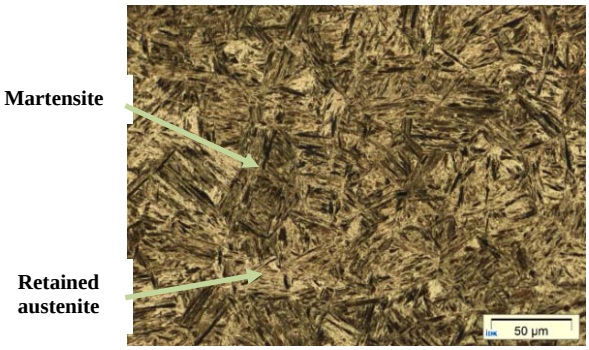

(b)

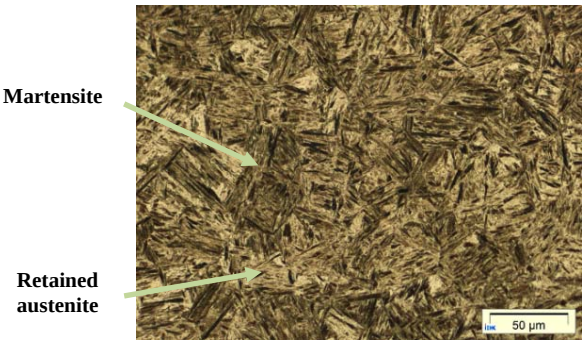

(c)

Figure 17. Comparing the microstructures of 22MnB5 after austenitizing and quenching with, (a) the austenization temperature of 900˚C, (b) the austenitization temperature of 1100˚C, and (c) the austenitization temperature of 1200˚C.

Figure 18 presents the microstructures near to the fracture areas of the samples where strain localisation occurred after hot tensile straining. Comparison between the microstructure of the samples after quenching without deformation and samples after deformation mostly shows martensitic phase in both cases, though some retained austenites were also observed, Figures 17 and 18.

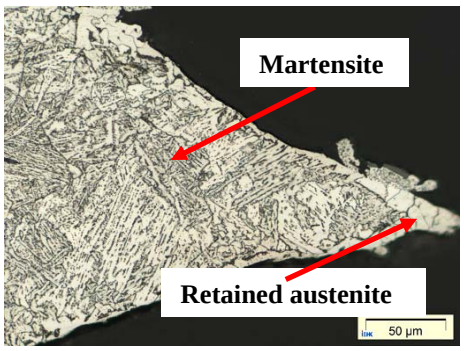

(a)

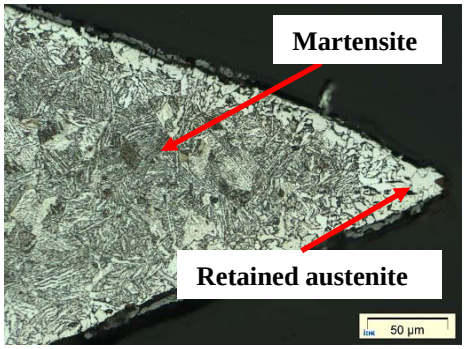

(b)

Figure 18. Comparing the microstructures of 22MnB5 after hot tensile testing at 1100˚C, (a) at strain rate of 0.001 s^{-1}, and (b) at strain rate of 0.1 s^{-1}

After hot tensile test, large voids were observed in some samples. Figure 19 (a) shows these porosities in the microstructure of the sample after hot tensile test at 1100°C and strain rate of 0.1 s^{-1}. The failure of this steel at high temperature is attributed to cup and cone fracture which is the feature of ductile fracture. The ductile fracture usually occurs in the low carbon steel. A slightly more homogeneous dimple structure was found in the sample failed at highest strain rate, as discussed in.[12] As a result, forming at high strain rate condition may have the tendency to produce a large dimple occurrence. Furthermore, the high temperature promotes the ductile fracture because of the FCC structure. In the results in Figure 7, the stress values decrease when the forming temperature increases. These results confirm that the ductile fracture will occur at high temperature. In addition, there is the high amount of retained austenite in the tip or the border area because this region is decarburized during cooling down by air, see Figure 19 (b).

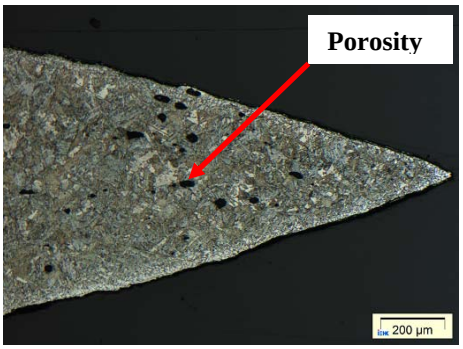

(a)

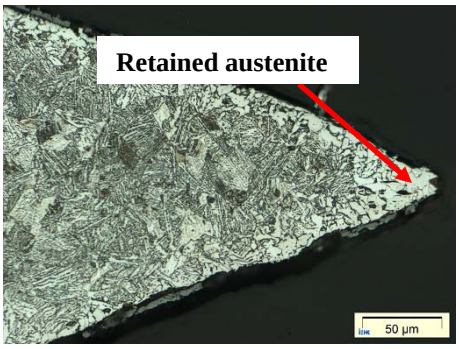

(b)

Figure 19. Microstructures of 22MnB5 after hot tensile test at 1100˚C and at strain rate of 0.1 s^{-1}, (a) 100x and (b) 500x

Conclusions

The determination of material behaviour at high temperature of steel grade 22MnB5 by using the hot tensile test and LSE system was presented. Stress-strain responses at different temperatures and strain rates were characterized. The local deformation and strain rate values were investigated. It can be concluded that this steel grade can provide very high strength properties after controlled cooling process.

Cooling rate, austenitization temperature, strain rate and chemical composition (i.e. carbon and boron) are the main factors that affect the mechanical properties and microstructure development. The martensite phase in the sample after hot deformation and quenching is finer at higher strain rate. In contrast to the hot forming at high temperature, the links of martensite are coarser than that of the lower temperature. Chemical composition is a factor that could be controlled by steel making process. The special element of 22MnB5 that promotes hardness and strength properties is boron.

The simulated force-displacement curves are in good agreement with the experimental results. FEM simulation is a useful method to display a first estimated result in the hot sheet metal working. Furthermore, the hot tensile test can provide reliable important mechanical properties of material at high temperature. The results from the hot tensile test can be used for the material design in the industrial manufacturing.

Acknowledgement

This work has been carried out under a collaborative research between RWTH Aachen University and the Sirindhorn International Thai-German Graduate School of Engineering (TGGS) at KMUTNB. The authors gratefully acknowledge the financial support of the Deutsche Forschungs-gemeinschaft (DFG) and the Research Fund for Coal and Steel of the European Community within the project RFSR-CT-2004-00034.

References

1. Naderi, M., Uthaisangsuk, V., Prahl, U. and Bleck, W. 2008. A numerical and experimental investigation into hot stamping of boron alloyed heat treated steels. *Steel Res. Int.* **79(2)** : 77-84.

2. Tackle, G., Forch, K.and Sartorious, A. 1993. Heat treatable and surface hardening steels for vehicle and machine construction. *Steel*, Vol.2 Applications, Springer-Verlag. :118-176.

3. Bleck, W. 2007. *Material Science of Steel; Text book for RWTH Students.* Department of Ferrous Metallurgy, RWTH Aachen University. : 165-166.

4. Kapadia, B.M.1978. *Hardenability concepts with application to steel.* Warrendale : A.I.M.E. : 448.

5. Morral, J.E. and Cameron, J.B. 1980. *Boron hardenability mechanisms.* The Metallurgical Society of the A.I.M.E.

6. Jonsson, M. Products in hot stamped boron steel, GESTAMP. www.autosteel.org.

7. Kapadia, B. 1977. Prediction of the boron hardenability effect in steel-A comprehensive review. *Hardenability concepts with applications to steel, Con.Proc.* Chicago, 24 – 26 Oct.: 448 – 482.

8. Naderi, M., Durenberger, L., Molinari, A. and Bleck, W. 2008. Constitutive relationships for 22MnB5 boron steel deformed isothermally at high temperatures. *J. Mater. Sci. Eng. A.* **478(1-2)** : 130-139.

9. Turetta, A., Bruschi, S. and Ghiotti, A. 2006. Investigation of 22MnB5 formability in hot stamping operations. *J. Mater. Process. Technol*. **177(1-3)** : 396-400.

10. Vadillo, L., Santos, M.T., Gutierrez, M.A., Pérez, I., González, B. and Uthaisangsuk, V. 2007. Simulation and experimental results of the hot metal gas forming technology for high strength steel and stainless steel tubes forming. In: *Proceeding of the 9th International Conference on Numerical Methods in Industrial Forming Processes*, June 17-21. Porto, Portugal : 1199-1204.

11. Nishiyama, Z. 1978. *Martensitic Transformation*. New York : Academic Press. : 28.

12. Vaynman, S., Fine, M.E., Lee, S. and Espinosa, H.D. 2006. Effect of strain rate and temperature on mechanical properties and fracture mode of high strength precipitation hardened ferritic steels. *Scr. Mater*. **55** : 351-354.